Biochimica et Biophysica Acta, 1099 (1992) 25–34

BBABIO 43541

Multifrequency EPR investigations into the origin of the S_2-state signal at $g = 4$ of the O_2-evolving complex

Alice Haddy [a,b], W. Richard Dunham [a], Richard H. Sands [a] and Roland Aasa [b]

[a] *Biophysics Research Division, University of Michigan, Ann Arbor, MI (U.S.A.) and* [b] *Department of Biochemistry and Biophysics, Chalmers University of Technology, Göteborg (Sweden)*

(Received 21 March 1991)
(Revised manuscript received 11 September 1991)

Key words: EPR; $g = 4$ signal; Multifrequency; Oxygen-evolving complex; Spin state; S_2-state

The low-temperature S_2-state EPR signal at $g = 4$ from the oxygen-evolving complex (OEC) of spinach Photosystem-II-enriched membranes is examined at three frequencies, 4 GHz (S-band), 9 GHz (X-band) and 16 GHz (P-band). While no hyperfine structure is observed at 4 GHz, the signal shows little narrowing and may mask underlying hyperfine structure. At 16 GHz, the signal shows g-anisotropy and a shift in g-components. The middle Kramers doublet of a near rhombic $S = 5/2$ system is found to be the only possible origin consistent with the frequency dependence of the signal. Computer simulations incorporating underlying hyperfine structure from an Mn monomer or dimer are employed to characterize the system. The low zero field splitting (ZFS) of $D = 0.43$ cm^{-1} and near rhombicity of $E/D = 0.25$ lead to the observed X-band g value of 4.1. Treatment with F^- or NH_3, which compete with Cl^- for a binding site, increases the ZFS and rhombicity of the signal. These results indicate that the origin of the OEC signal at $g = 4$ is either an Mn(II) monomer or a coupled Mn multimer. The likelihood of a multimer is favored over that of a monomer.

Introduction

The formation of O_2 from H_2O in higher plants and algae proceeds via a four-step oxidation of the oxygen-evolving complex (OEC). Classical studies of oxygen yield in response to a train of light flashes have been described by a series of S-states (S_0 through S_4) with S_1 or a combination of S_1 and S_0 as the initial dark-adapted state and S_4 as the state in which oxygen is evolved [1]. The four Mn atoms associated with the OEC [2,3] probably change oxidation state during at least two of the S-state transitions, including the S_1-to S_2-state change, but little is known of the details.

The chemical nature of the S_2-state has been partially characterized through two low-temperature X-band EPR signals, for which association with the S_2-state was demonstrated by studies of flash oscillation of the signal intensity [4,5]. The signal centered at $g = 2$, with a multiline structure indicative of a cluster of Mn ions, was suggested to be in the configuration of either a dimer [4,6], a trimer [7] or a tetramer [8,9]. The second signal appears as a single broad line centered at about $g = 4.1$ [10,11]. Although this signal lacks EPR structure, two lines of evidence indicate that it also arises from Mn. The first of these is an X-ray absorption near edge (XANE) study in which a shift in the Mn K-edge, showing the oxidation of Mn, was observed in PS II preparations under the same conditions which induce the $g = 4$ EPR signal [12]. More recently, the NH_3-modified signal at $g = 4$ from oriented PS-II-enriched membranes was found to show a hyperfine structure consistent with an Mn multimer [13].

The two signals are not always observed under the same experimental conditions, and their intensities appear to be mutually exclusive. Illumination of dark-adapted samples at lower temperatures (130–140 K) produces mostly the signal at $g = 4$, while illumination

Abbreviations: Chl, chlorophyll; DCBQ, 2,5-dichloro-*p*-benzoquinone; DCMU, 3-(3,4-dichlorophenyl)-1,1-dimethylurea; EPR, electron paramagnetic resonance; Hepes, 4-(2-hydroxyethyl)-1-piperazineethanesulfonic acid; Mes, 4-morpholineethanesulfonic acid; OEC, oxygen-evolving complex; PPBQ, phenyl-*p*-benzoquinone; PS II, Photosystem II; ZFS, zero field splitting; XANE, X-ray absorption near edge.

Correspondence (present address): A. Haddy, Hematology Research, Mayo Clinic, Rochester, MN 55905, U.S.A.

at higher temperatures (around 200 K) favors the multiline signal [11,14]. When illumination is at 200 K, both signals are observed in PS II samples prepared with sucrose as cryoprotectant, while samples containing glycerol, ethylene glycol or ethanol show only the multiline signal, with enhanced intensity and definition [5]. Furthermore, treatment with F^- or NO_3^- induces the signal at $g = 4$ with little or no multiline signal remaining [11,15].

There is general concurrence based on several lines of evidence that the multiline and $g = 4$ signals arise from separate populations of PS II centers and therefore represent different states of the same site [5,16,17]. While this explains their mutually exclusive relationship, the chemical origin of the two signals and how they are interrelated is still in question. One group has suggested that the signal at $g = 4$ is due to an Mn(IV) monomer in redox equilibrium with an Mn cluster [16]. Another group has suggested that both the multiline and $g = 4$ signals arise from the same Mn cluster in different conformations [9]. This is supported not only by the previously mentioned study of NH_3-treated oriented membranes [13], but also by a study in which the appearance of the multiline and F^--induced $g = 4$ signals are associated with the same change in magnetic susceptibility [18].

In the present work, an EPR study of the S_2-state signal at $g = 4$ involving three microwave frequencies has been undertaken to elucidate further spectroscopic details of the signal. By expanding the frequency range of study, hyperfine or g value contributions may be brought out and the signal can be characterized with greater certainty. In this study, little change in the $g = 4$ signal was observed at lower S-band (4 GHz) frequency. At higher P-band (16 GHz) frequency, the signal showed g value anisotropy and broadening. The characteristics of the P-band signal, as well as its response to likely ligands, strongly support an $S = 5/2$ system as its origin. The spectra are analyzed in terms of both monomer and coupled Mn multimer systems.

Materials and Methods

PS-II-enriched thylakoid membranes were prepared from spinach by the Triton X-100 extraction method of Berthold, Babcock and Yocum [19], as modified by Franzén et al. [20]. Preparations were stored in liquid N_2 at a concentration of 10–20 mg Chl/ml in buffer containing 20 mM Mes (pH 6.3), 15 mM NaCl, 5 mM $MgCl_2$ and 0.4 M sucrose. O_2-evolving activity was 600 ± 100 μmol O_2/(mg Chl h^{-1}) at 25°C using a Clark-type O_2 electrode with PPBQ or DCBQ as acceptor.

PS II core complex samples were prepared by a modification of the method of Ghanotakis et al. [21] as described previously [22]. O_2-evolving activity was 1600 $\pm$ 100 μmol O_2/(mg Chl h^{-1}) at 25°C using a Clark-type O_2 electrode with DCBQ as acceptor.

PS-II-enriched membranes were oriented by partially dehydrating them onto mylar sheets under a stream of N_2 gas at 4°C, as described previously [22]. The mylar sheet was cut into strips 2.5 mm wide before dabbing with dark-adapted PS-II-enriched membranes. After dehydrating, eight 3-cm-long pieces of PS-II-laden mylar were sandwiched together under green light and placed at the bottom of an EPR tube. The sample was dark-adapted for 30 min and stored in liq N_2.

F^--washed PS-II-enriched membranes were prepared by suspension in 20 mM Mes (pH 6.3), 25 mM NaF, and 0.4 M sucrose to a concentration of 1–1.5 mg Chl/ml, and centrifuging at 20000 rpm for 10 min. This wash was repeated once. The concentrated sample was placed in an EPR tube and dark adapted for 1 h before freezing. O_2-evolving activity, measured as described above in the F^--containing buffer, was about 20% of the control.

For ammonia binding in the S_1-state, the pH of PS-II-enriched membranes was first elevated by washing once in 20 mM Hepes (pH 7.5), 15 mM NaCl, and 0.35 M sucrose. After dark adapting for about 2 h, 150 μM DCMU in dimethyl sulfoxide solvent and 60 mM $(NH_4)_2SO_4$ were added sequentially in the dark and the sample was frozen 1 min later. A control sample was prepared in the same way except with Na_2SO_4 in place of $(NH_4)_2SO_4$.

Each EPR spectrum shown represents the difference between the illuminated and dark-adapted sample. For samples containing ethanol, the indicated volume of 95% ethanol was added to the dark-adapted sample 1–2 min before freezing. The S_2-state was prepared by illuminating at 200 K in a solid CO_2/ethanol bath for the times indicated in the figure legends. Illumination was carried out using incandescent light from a 300 W tungsten source passed through 7 cm of a 10 mM $CuSO_4$ solution or, in the case of S-band studies, from a 250 W source passed through 10 cm of water and an infrared filter; the resultant intensity was 2000 W/m^2 at the sample in both cases. For S-band experiments, the sample volume was about 1.5 ml because of the large EPR cavity employed. For X- and P-band experiments, the sample volume was about 0.3 ml; the same sample was used at both frequencies.

X-band (9.2 GHz) EPR spectroscopy was performed using a Varian E-line spectrometer with an E102 microwave bridge. S-band (3.9 GHz) EPR spectroscopy was performed using a Bruker ER 200D-SRC spectrometer equipped with an ER 061 SR microwave bridge and an ER 6102 SR reentrant cavity, as described previously [22]. P-band (15.5 GHz) EPR spectroscopy was performed using a homebuilt spectrometer, described by Stevenson [23], which employed a

Varian VA94 klystron tube as microwave source and a cylindrical cavity operating in the TE011 mode. For X- and P-band experiments, the data were digitized on a Tracor Northern digital signal averager interfaced to a personal computer. The modulation frequency was 100 kHz for X- and P-band experiments and 12.5 kHz for S-band. Cryogenic temperatures were maintained using helium flow systems designed by Oxford Instruments (model ESR-9) for S-band experiments or in-house for X- and P-band.

Relative spin quantitations of the multiline and $g = 4$ signals were carried out by integration of the X-band signals. The narrow radical at the center of the multiline signal (Tyr D^+ and Tyr Z^+) was replaced with baseline prior to integration. The multiline signal was not corrected for other light-induced signals because these were assumed to be unaffected by ethanol. Differences in transition probability were accounted for as described by Aasa and Vänngård [24] assuming $g = 2.0$ for the multiline signal and $g = 4.1$ for the signal at $g = 4$.

Spectral syntheses were carried out on IBM-compatible personal computers using Fortran programs (Dunham, W.R., unpublished data; Haddy, A., unpublished data). Calculation of effective principal g values for $S = 3/2$ and $S = 5/2$ systems was performed using a program which diagonalizes the spin Hamiltonian matrix based on a given magnetic field strength, zero field splitting D and rhombicity E/D, and assuming a true g value of 2.000 except where otherwise stated. The program used for simulations of EPR spectra was written for effective spin $S' = 1/2$ systems with nuclear hyperfine coupling and Gaussian lineshape.

Results

Multifrequency data

The $g = 4$ EPR signal induced in PS-II-enriched thylakoid membrane preparations by illumination at 200 K was studied at three microwave frequencies: 3.9 GHz (S-band), 9.2 GHz (X-band), and 15.5 GHz (P-band) (Fig. 1, top curves). As in other studies, at X-band frequency the signal appeared as a single broad line centered at $g = 4.1$ with a linewidth of 34–36 mT. Upon lowering the frequency to S-band, little change was found; the signal showed about the same g value and no hyperfine structure became apparent. Observed S-band linewidths were somewhat narrower than X-band, ranging from 27 to 35 mT. Upon increasing the frequency to P-band, however, the $g = 4$ signal changed in shape in a manner consistent with the partial resolution of two g value components. The overall signal appeared to widen to about 70 mT from peak to trough, with the point of baseline crossover at about $g = 3.85$.

To test whether the apparent anisotropy of the signal at $g = 4$ represented a powder pattern from a single center or two signals from different centers, a partially oriented membrane sample was examined at P-band. The degree of orientation, as judged from the cytochrome *b*-559 g_x and g_z resonances, was found to be good; however, a small amount of each peak remained at the orientation for which it would have been absent given optimal orientation (see Ref. 25, for example). Using this preparation, two components of the signal at $g = 4$ were partially differentiated by changing the angle between the membrane normal and the magnetic field direction. At an orientation of 0°, a signal with intensity above and below the baseline appeared with a baseline-crossover at about $g = 3.85$ (Fig. 2, top). At 90° a signal with intensity mostly above the baseline appeared with the peak at about $g = 4.7$ (Fig. 2, bottom). These data indicated that the signal at $g = 4$ arose from a single spin system with pronounced g-anisotropy.

Simulations of the signal at $g = 4$

Several features, based on these and previous observations, must be accounted for in an adequate model for the signal at $g = 4$. At the lowest frequency, S-band, the overall linewidth in terms of field units did not narrow as expected if 'g-strain' broadening were the principal determinant of linewidth. This indicated that the narrowing of the signal was limited to a linewidth about equal to that observed at S-band. A likely source for this would be underlying hyperfine structure, which would be expected for a signal arising from Mn.

A more difficult observation to explain was the g-anisotropy observed at P-band, which was great enough that two of the g-components apparently differed by about 0.85. This anisotropy is obscured at X-band frequencies, although some anisotropy can be observed in oriented samples [25]. Comparison of the X- and P-band signals indicated that the higher field portion of the signal moved to a lower g value as the frequency increased. Early simulation attempts showed that a single set of g values could not simulate the data at all three frequencies, regardless of linewidths used.

Zero field splitting (ZFS), which is the principal determinant of the high g values observed, is also likely to be responsible for the frequency dependence of the signal. Thus, several possible half-integral spin systems with $S > 1/2$ were considered for the origin of the S_2-state signal at $g = 4$. Possible model spin systems were tested by calculating the theoretical g values from the ZFS parameters by a matrix diagonalization procedure. An axial $S = 3/2$ system, which shows powder patterns with $g_{x,y,z} = 4, 4, 2$, seemed to be a likely possibility, since a departure from axial symmetry could cause a separation of the two low-field g-compo-

nents. This type of spin system has been proposed previously for the S_2-state signal at $g = 4$, with its source in either a Mn multimer [9] or an Mn(IV) monomer [16].

Attempts to simulate the X-band signal at $g = 4$ using the g values observed at P-band (4.7 and 3.85), which would correspond to a high ZFS situation,

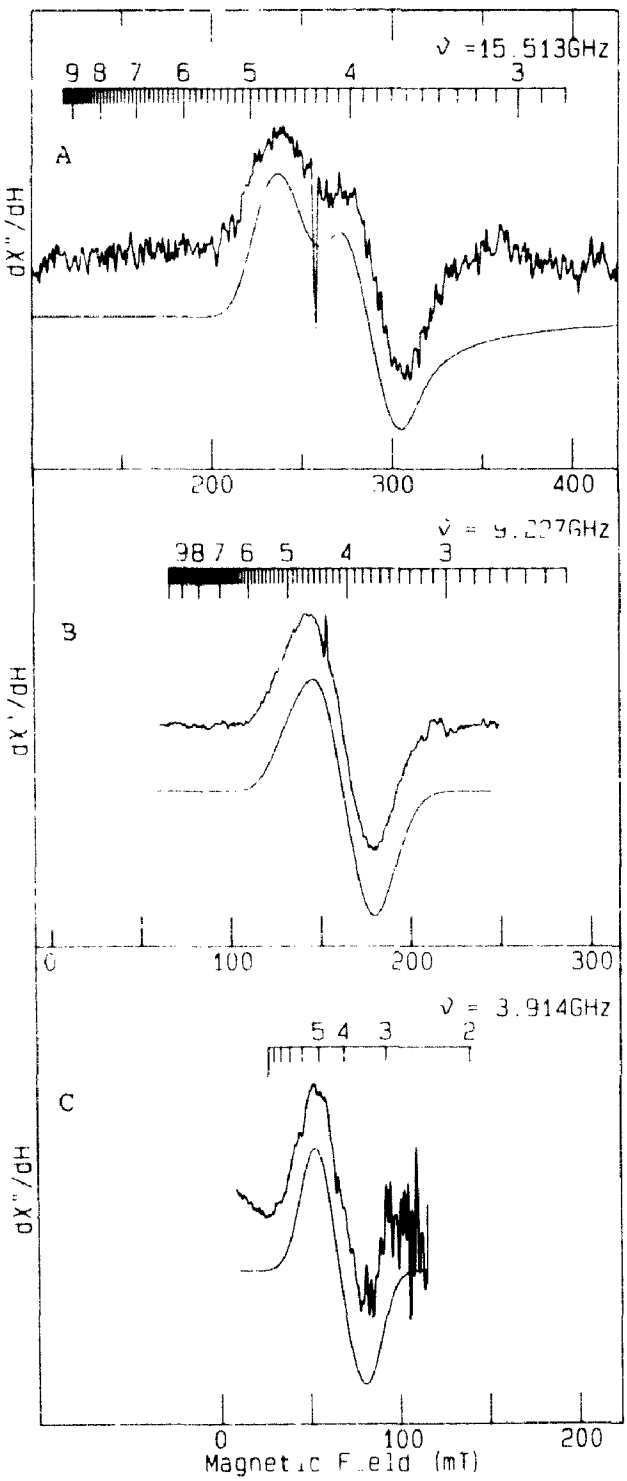

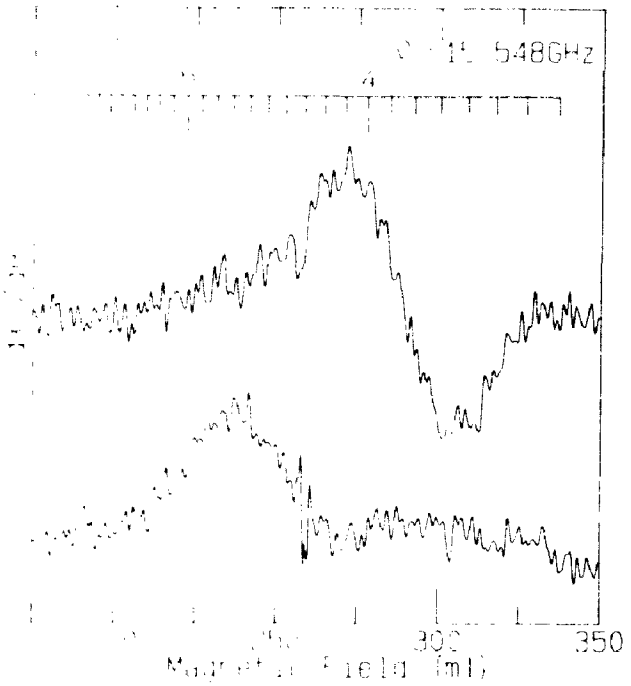

Fig. 2. P-band signal at $g = 4$ from oriented PS-II-enriched membranes, with angles between the membrane normal and the magnetic field direction of 0° (top) and 90° (bottom). The oriented membrane sample, prepared as described in Materials and Methods, was illuminated for 4 min after taking spectra in the dark-adapted state. EPR conditions were as described for the P-band experiment in the legend to Fig. 1.

showed that a near axial $S = 3/2$ system would not produce the proper lineshape (Fig. 3). Simulated signals were generally too broad from peak to trough and showed either a pronounced shoulder (Fig. 3, dashed line) or, if wider linewidths were used, a lopsided signal (Fig. 3, dotted line). In addition, all X-band $S = 3/2$ simulations showed greater asymmetry with respect to areas above and below the baseline than the

Fig. 1. Comparison of the low-temperature S_2-state EPR signal at $g = 4$ from PS-II-enriched membranes at three microwave frequencies (A) P-band, 15.5 GHz; (B) X-band, 9.2 GHz; and (C) S-band, 3.9 GHz. The spectra show the same span in magnetic field units and coincide at $g = 4.1$. Top curves, experimental spectra: The P- and X-band spectra were taken on the same sample (11 mg Chl/ml); it was illuminated for 5 min for the P-band and, after redark-adapting, for 6 min for the X-band experiment. The S-band sample (20 mg Chl/ml) was illuminated for 32 min. Microwave power and modulation amplitude were 2 mW and 1.3 mT, respectively, at P-band, 20 mW and 1.6 mT at X-band, and 20 mW and about 0.9 mT at S-band. Temperature was 11 K for X- and P-band experiments and 10 K for S-band. Discontinuities at $g = 4.3$ resulted from subtraction of the narrow line attributed to rhombic Fe(III). The S-band spectrum shows overlapping lines from the multiline signal. Bottom curves, simulated spectra: Spectral syntheses were carried out as described in the text using the effective g values calculated for an $S = 5/2$ system with $D = 0.43$ cm^{-1} and $E/D = 0.25$ (see Table I) and assuming underlying hyperfine coupling to a nuclear spin $I = 5/2$ system with $A = 4.5$ mT.

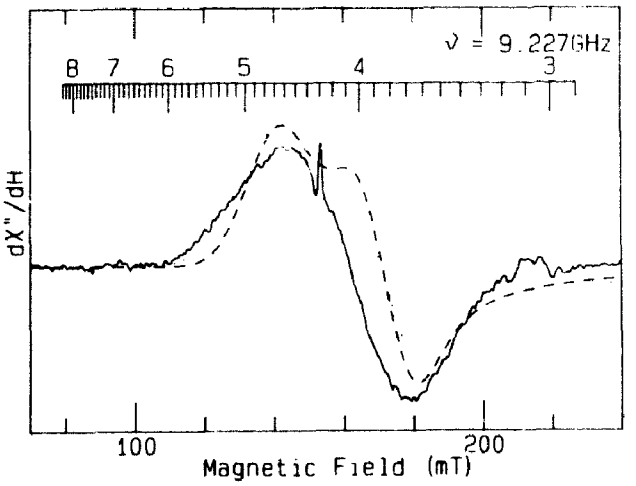

Fig. 3. Simulation of the X-band signal at $g = 4$ assuming a near axial $S = 3/2$ system. Solid line: experimental spectrum taken from Fig. 1B, top curve; dashed and dotted lines: simulations carried out setting $g_{x,y,z} = 4.68, 3.82, 2.00$ and linewidths $W_{x,y,z} = 17.5, 15, 20$ mT and 22.5, 20, 25 mT, respectively.

experimental spectrum because of the appearance of only two of the three powder pattern components in the $g = 4$ region. Except for the unmodified P-band signal observed here, previously published spectra as well as our own appear to be full derivative-shaped signals.

Examination of the theoretical basis for a near axial $S = 3/2$ source for this signal revealed further potential problems. Simulations employing the expected true g value (g_{tr}) of 2.0 could produce neither the effective g values nor the frequency dependence required by the data. We found that the lowest g_{tr} that could produce the observed P-band g values was 2.15 using a high ZFS of $D = 3.0$ cm^{-1} (or greater) and $E/D = 0.066$. With this high ZFS there is almost no frequency dependence of the signal. A system in which the ZFS was lower, with $D = 0.60$ cm^{-1} and $E/D = 0.062$, and the true g value higher, $g_{tr} = 2.22$, also produced the P-band g values. This ZFS is low enough to show frequency dependence, but simulations were not satisfactory. First, although the effective X-band g values of 3.96 and 4.79 produced a signal with a baseline crossover near $g = 4.0$ and mid-peak around $g = 4.1$, the shape of the signal again did not match the observed signal. In addition, the corresponding S-band g values increased unlike the observed signal. Another result of these high g_{tr} values would be a parallel resonance near $g = 2.15$–2.2, where it would be more noticeable than the usual $g = 2$ parallel resonance. Finally, there is no satisfactory physical explanation for these g_{tr} values from an Mn source. The high angular momentum implied by such a high g_{tr} is lacking even for Mn(III) which shows at most $g = 2.01$ as its perpendicular resonance. For these reasons, an axial $S = 3/2$ system is not consistent with the S_2-state signal at $g = 4$.

TABLE I

Parameters used for simulation of the S_2-state signal at $g = 4$ assuming underlying hyperfine structure from an Mn monomer

Parameter [a]	S-band (3.91 GHz)	X-band (9.23 GHz)	P-band (15.5 GHz)
g value	3.73	3.63	(0)
	4.05	3.98	3.83
	4.78	4.75	4.68
Width (mT)	15	20	(20)
	15	15	17.5
	15	17.5	17.5

[a] Parameters correspond to the simulations shown in Fig. 1, bottom curves. The g values were calculated for a near rhombic $S = 5/2$ system for which $D = 0.43$ cm^{-1} and $E/D = 0.25$. Underlying hyperfine structure from an $I = 5/2$ nucleus with $A = 4.5$ mT was included in the simulations. The widths given are for the individual hyperfine lines; their choice was therefore influenced by the hyperfine splitting used.

The signal at $g = 4$ was found to fit a model attributing its origin to the central Kramers doublet of a rhombic $S = 5/2$ system. This model provided g values and frequency dependences required by the data assuming $g_{tr} = 2.000$. The g values which best fit the data were correlated with a ZFS, D, of 0.43 cm^{-1} and a rhombicity, E/D, of 0.25 (Table I), where D and E are defined in the spin hamiltonian ZFS term, $[D(S_z^2 - S(S+1)/3) + E(S_x^2 - S_y^2)]$. Although the g values calculated are very sensitive to changes in D, the errors in D and E/D may be up to 10% due to factors which influence lineshape (see below). The observed X-band g value of 4.1, rather than 4.3 observed for many rhombic $S = 5/2$ systems, can be attributed primarily to the rhombicity E/D of 0.25, which is low compared to 1/3 for complete rhombicity. The frequency dependence of the effective g values results from the low ZFS energy relative to the Zeeman energy (Fig. 4). One of the more notable results of this analysis is that, because of the low value of D, one of the three principal axes no longer shows a relevant energy transition at P-band.

While the simulations presented here reproduced the g values and overall appearance of the signal well at all three frequencies, the lineshapes produced are not expected to be accurate, especially for the P-band signal. In particular, the method used to calculate the angular dependence of g values and transition probabilities based on principal axis values is an approximation which becomes less accurate for the P-band spectrum. Simulations of the P-band signal, which employed $g = 0$ as one of the principal g-components, show lineshape inaccuracies that probably arise from this assumption. In addition, the use of a Gaussian

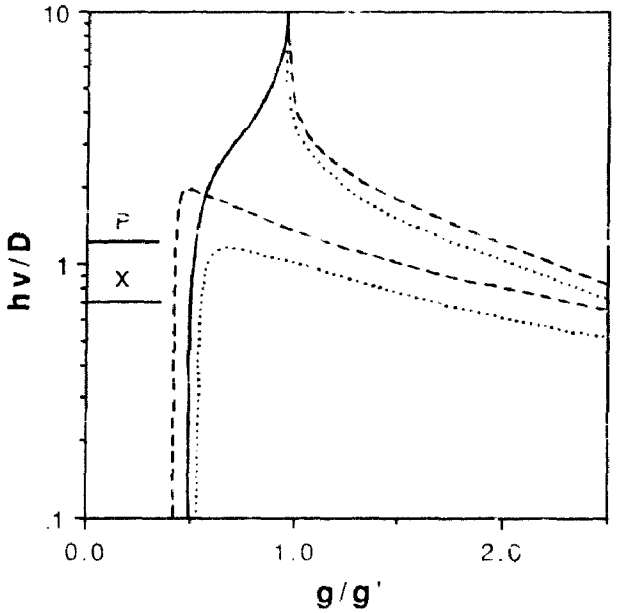

Fig. 4. Transition frequency as a function of effective g value for the unmodified S_2-state signal at $g = 4$. The calculated data are plotted as $\log(h\nu/D)$ vs. g/g', where g' is the effective g value and $g = 2.000$. Transitions along the three principal axes are shown for the middle Kramers doublet of an $S = 5/2$ system in which $E/D = 0.25$. Bars indicate the X- and P-band transitions for the case in which $D = 0.43\ cm^{-1}$. (After Ref. 35.)

lineshape becomes problematic as the g value increases because it is relevant to an energy scale rather than a g-scale. Lineshapes are expected to appear distorted at lower field as a result of 'g-strain' [26].

Simulations of the signals included hyperfine coupling to one Mn nucleus ($I = 5/2$) (Fig. 1, bottom curves) or to an Mn dimer. Underlying hyperfine splitting accounted for the frequency independent linebroadening and provided an estimate of the largest splitting that would not affect the resolution of g-anisotropy at P-band. Isotropic hyperfine coupling to a single Mn nucleus fit the data well with $A = 4$–5 mT. To simulate an underlying multimer hyperfine pattern while keeping the computation time at a minimum, a dimer model in which one coupling constant was twice that of the other was used. Isotropic constants no greater than $A_1 = 2.5$ and $A_2 = 5$ mT could be incorporated without distorting the shape of the P-band signal. The line spacing of this 16-line pattern was smaller than the 3.6 mT spacing observed by Kim et al. [13]. The difference might be due to either the different forms of the signal (NH_3-modified vs. unmodified) or a difference in the pattern of line intensity between the simulated and true signals.

Evidence supporting an $S = 5/2$ origin

Rhombic $S = 5/2$ systems can show one or two signals at $g = 9$–10 arising from the upper doublet of one principal axis and/or the lower doublet of another principal axis. The signal has a relatively low transition probability, but is generally narrow. For the $S = 5/2$ system described here, signals are expected to appear at $g = 9.2$ and/or $g = 9.8$ assuming $g_{tr} = 2.0$, with the former having the greater transition probability. We were not successful in observing an appropriate X-band signal at $g = 9$–10. Although some light-induced features were observed, the sensitivity to ethanol and F did not match that of the signal at $g = 4$. The $g = 9$–10 region of the spectrum also contains a signal from rhombic Fe(III) which may interfere with observation of a light-induced signal. In addition hyperfine splitting from Mn would reduce the likelihood of resolving individual lines. These potential problems, in addition to the expected low transition probability, probably explain the lack of observing an S_2-state signal at $g = 9$–10.

One way of testing the $S = 5/2$ identity of the signal at $g = 4$ depends upon the apparent exchange of spin population with the multiline signal at $g = 2$ in response to ethanol. Spin population from the multiline signal ($S = 1/2$ [16]) would redistribute over three Kramers doublets, of which only one would be observed, upon conversion of the center to an $S = 5/2$ state. Thus we compared the gain of multiline signal to the loss of the signal at $g = 4$ due to the presence of ethanol in otherwise equivalently prepared samples. The integrated intensity of the two S_2-state signals were studied at X-band for pairs of samples, with and without 6% ethanol, from two PS-II-enriched membrane preparations and a core complex preparation. The difference spectra of these samples showed even baselines and therefore gave reasonably accurate integrated intensities. After correction of the signal intensities for the difference in transition probabilities [24], the ratio of the loss in $g = 4$ signal to the gain in multiline signal intensity was found to be an average of 0.36 due to the presence of ethanol (0.38, 0.35 and 0.34 for the three preparations, respectively). This is close to the expected value of 0.33 for an $S = 5/2$ system that exchanges spin population with an $S = 1/2$ system.

F^-- and NH_3-modified signals at P-band

The $g = 4$ region was further studied at P-band frequency using PS-II-enriched membranes in which NaCl had been replaced with NaF. F^- is known to enhance the intensity of the signal at $g = 4$ while greatly reducing the intensity of the multiline signal [11,15]. As expected, the signal at $g = 4$ increased significantly after this treatment (Fig. 5), approximately doubling as a result of the replacement of NaCl with NaF. In addition, the observed anisotropy of the signal at 15.5 GHz was lower than that of control samples.

Good simulations of the F^--modified signal were obtained using the g values corresponding to $D = 0.53$

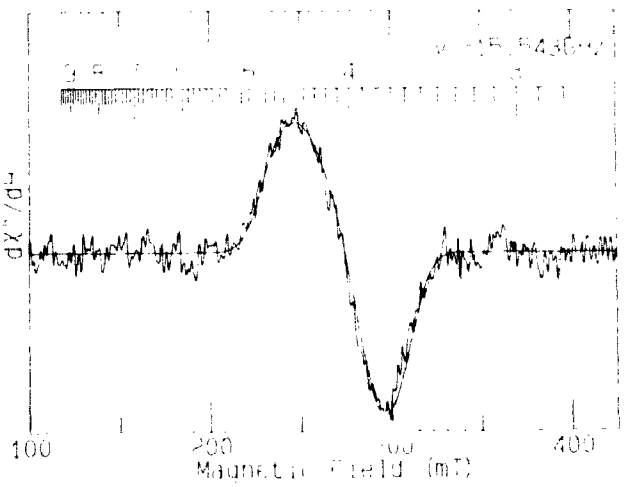

Fig. 5. P-band signal at $g = 4$ of F^--treated PS-II-enriched membranes. The F^--treated sample (13 mg Chl/ml), prepared as described in Materials and Methods, was illuminated for 5 min. Experimental conditions were as described for P-band in the legend to Fig. 1. The simulation shown is for a system with $g_{x,y,z} = 3.71, 4.02, 4.59$; $W_{x,y,z} = 17.5, 22.5, 17.5$ mT and $A = 4.5$ mT for an $I = 5/2$ nucleus.

cm^{-1} and $E/D = 0.27$. With these higher values of D and E, resonances corresponding to all three principal axes are observed in the $g = 4$ region. Hyperfine coupling of 2.5 to 6 mT to a nucleus of $I = 5/2$ could be incorporated with varying linewidths. The possibility that F^- induced a second signal in addition to the control signal was eliminated since the additional signal would have had an unnatural appearance. Thus the effect of F^--modification on the signal at $g = 4$ was to increase both the ZFS, D, and the rhombicity, E/D, of the $S = 5/2$ center.

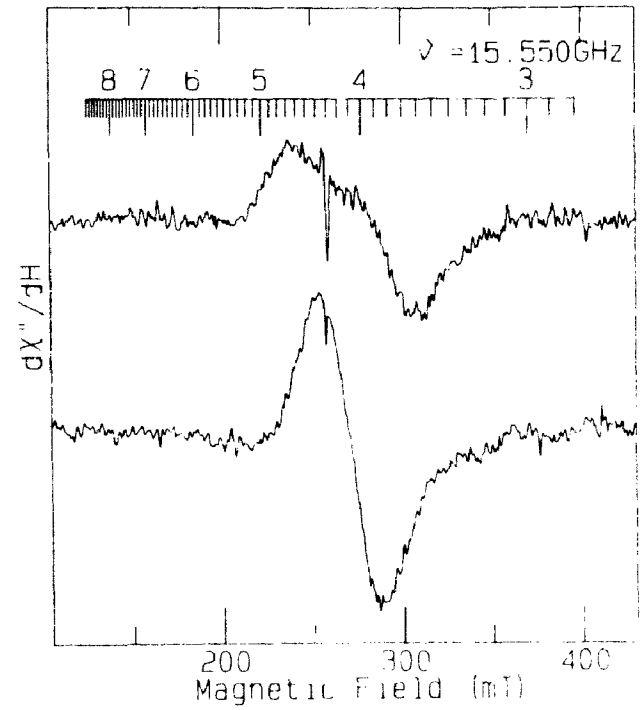

Fig. 6. Effect of NH_3 binding in the S_1-state on the S_2-state P-band signal at $g = 4$. 60 mM Na_2SO_4 (top) or $(NH_4)_2SO_4$ (bottom) was added to dark-adapted PS-II-enriched membranes (15 mg Chl/ml) at pH 7.5, as described in Materials and Methods. The S_2-state was achieved by illumination at 200 K for 5 min. EPR conditions were as described for P-band in the legend to Fig. 1

NH_3 binding to the OEC has been found to affect the signal at $g = 4$ [27,28]. This results from NH_3 binding in both the S_1- and S_2-states, although it is more pronounced in the latter. The effect of NH_3 binding in the S_1-state on the $g = 4$ signal was observed at P-band frequency. $(NH_4)_2SO_4$ was added to dark-adapted PS-II-enriched membranes at an elevated pH to allow binding in the S_1-state, then the S_2-state was produced by illumination at 200 K. A single symmetrical line at $g = 4.1$ was found after this treatment (Fig. 6, bottom), while the Na_2SO_4-containing control showed the same anisotropic signal as untreated samples (Fig. 6, top). The integrated intensity of the NH_3-modified and control signals were similar with only about a 10% decrease in the NH_3-treated signal. Simulations showed that this form of the signal at $g = 4$ corresponded to $D = 0.44$ cm^{-1} and $E/D = 0.30$, with the entire powder pattern observable as for the F^--treated sample.

Discussion

Characteristics of the multifrequency data

P-band frequency (15.5 GHz) EPR of the S_2-state signal at $g = 4$ from PS-II-enriched membranes has revealed that it is composed of at least two apparent g values separated by about 0.85 (Fig. 1A, top curve). Study of membrane samples prepared on mylar sheets showed that these g values corresponded to different components of one signal (Fig. 2). At P-band the g-components of the oriented signal were well separated, with the higher field component appearing at 0° between the membrane normal and the magnetic field direction. An orientation-dependent shift in the X-band signal at $g = 4$ was observed previously in similar preparations by Rutherford [25], although with little resolution of g-components.

At the lower S-band frequency (3.9 GHz), the signal at $g = 4$ resembled the X-band signal, with some slight narrowing. It showed no hyperfine structure, as an Mn signal might if individual linewidths decreased with frequency. But neither did the signal as a whole become notably narrower as it would if 'g-strain' broadening dominated the overall linewidth. This indicates a limit to the narrowing of the signal which is consistent with an underlying hyperfine structure. The g-anisotropy of the signal may contribute to difficulty in resolving individual lines at the lower frequency.

Spin state origin

One of the most interesting findings of this study was that a single set of g values, which would be appropriate for treatment of an isolated doublet, could not account for the data from all three frequencies. The relatively high g values and their variations with frequency indicated that zero field splitting (ZFS) played an important role and was low enough to account for frequency dependence. In addition, if the signals were not from the ground doublet of a Kramers system, the ZFS would have to be small enough for the signal to follow the Curie law above 4 K, as observed in previous studies [9,16].

Several possible origins of the signal were considered before choosing $S = 5/2$ as the model for simulations. The axial $S = 3/2$ system, which gives rise to a signal of the type $g_{x,y,z} = 4, 4, 2$, was investigated thoroughly before concluding that it was not a satisfactory model (see Results). The possibility that the signal at $g = 4$ might arise from an $S = 3/2$ state analogous to that of the octahedral d^7 ion Co(III), which shows a signal at $g = 4.3$ [29], was ruled out because of the unlikely electron configuration for Mn and the probable lack of frequency dependence. The higher spin states, $S = 7/2$ and $S = 9/2$, were also ruled out. The $S = 7/2$ state does not show an isotropic line at low field, although it often shows an axial signal of the type $g_{x,y,z} = 8, 8, 2$ from the ground Kramers doublet. The rhombic $S = 9/2$ system shows an isotropic low field signal from the middle Kramers doublet but with higher g values, typically $g = 6.36$ for high D and $E/D = 1/3$ or slightly lower. Some examples of this have been observed from synthetic tetranuclear Mn complexes with accompanying resonances near $g = 2$ and $g = 9$ [30].

The near rhombic $S = 5/2$ system, which successfully accounted for the g values and frequency dependences observed here for the signal at $g = 4$ (Fig. 1, bottom curves and Table I), is one of the most well documented spin systems. It is usually exemplified by highly rhombic Fe(III) with large ZFS in glasses and biological systems where transitions within the middle Kramers doublet appear as sharp signals at $g = 4.3$. Mn(II) in glasses also shows signals at $g = 4.3$ [31,32], but there are few if any reports of this in enzyme systems. The $S = 5/2$ system studied here was unusual in having a relatively low rhombicity and ZFS, which lead to the observed X-band g value of 4.1 and marked frequency dependence. The characteristics of the signal are such that at frequencies above P-band the two higher-field g-components are expected to disappear altogether. The remaining g-component would decrease in value where the line of Fig. 4 is nonvertical and become difficult to observe due to 'ZFS-strain', which can be thought of as an increase in $dg/d(h\nu/D)$. When nearing the limit of $g' = 2$, where the lines become vertical again, the signal would be difficult to distinguish from others. This explains, at least in part, why the signal at $g = 4$ was not observed in an earlier study at 35 GHz (Hansson, Ö, personal communication).

The expected temperature dependence of the signal from the middle Kramers doublet was calculated for the $S = 5/2$ system described here between 4 and 25 K and found to agree with previous experimental results [9,16]. Only minor departure from Curie law behavior is expected unless the temperature is below 2 K.

Spin density exchange with the multiline signal

The relative intensities of the multiline and $g = 4$ signals are influenced by a number of experimental factors including the cryoprotectant, the presence of ethanol, the temperature of illumination and the presence of certain anions such as F^- and NO_3^- [5,15]. With changes in these conditions, one signal appears to gain or lose intensity at the expense of the other. Although this observation has been made by numerous investigators, only one previous study [16] has carried out a spin quantitation of the apparent exchange.

For the redistribution of spin from an $S = 1/2$ system (multiline) to an $S = 5/2$ system ($g = 4$ signal) one would expect the $S = 5/2$ signal (which arises from one of three Kramers doublets) to gain about 1/3 of the multiline signal population lost by the $S = 1/2$ center. The samples studied with and without ethanol showed an average ratio of $g = 4$ signal gained to multiline signal lost of 0.36. A similar experiment described by Hansson and coworkers [16] gave a similar result: if the spin density observed at $g = 4$ is assumed to arise from an isotropic signal, then the loss of 1 spin of multiline signal correlates with the gain of 0.28 spin of $g = 4$ signal. The analysis presented here assumed that any spin intensity lost by the multiline signal in one or more $S = 1/2$ states corresponded to a gain in the $g = 4$ signal. It relied upon accurate integration of the signals, which can be difficult for difference spectra from cryogenic samples. While this analysis does not confirm the identity of the $g = 4$ signal as arising from an $S = 5/2$ state, it is consistent with this interpretation.

Source of the $S = 5/2$ signal

A Mn(II) monomer source for the signal at $g = 4$, although possible based solely on the observations made here, is unlikely when considering results from other laboratories. Most notable is the recent observation of hyperfine structure on the NH_3-modified $g = 4$ signal from oriented PS-II-enriched membranes [13]. Another recent study showed that the magnetic susceptibility change upon S_1- to S_2-state transition was the same during formation of both the multiline signal and the F^--induced $g = 4$ signal, indicating that the $g = 4$ sig-

nal arises from a cluster similar to the multiline signal [18]. Furthermore, XANE results which show a high average oxidation state (Mn(III) to Mn(IV)) in the $g = 4$ signal-associated S_2-state [12] do not support the presence of Mn(II). The lack of Mn oxidation in the S_2- to S_3-state transition [12,18] underscores the need for a high Mn oxidation state in the S_2-state so that water can be oxidized on subsequent steps.

A Mn cluster of nuclearity 3 or 4 offers a more satisfactory explanation for the signal at $g = 4$ than a dimer. The higher nuclearities appear more likely to produce an $S = 5/2$ ground state since a dimer (i.e., Mn(III)Mn(IV)) would be expected to couple strongly to produce an $S = 1/2$ ground state. In addition the higher nuclearities of 3 and 4 are more likely to show a reduction in line spacings from the monomer values, as noted by Kim and coworkers in their study of NH_3-treated oriented membranes [13].

F^-- and NH_3-modified signals

The F^-- and NH_3-modified P-band signals at $g = 4$ were found to have much lower g-anisotropy than the unmodified signal due to greater ZFS and rhombicity. The major difference between the two modified signals was that the replacement of Cl^- with F^- approximately doubled the spin concentration, whereas NH_3-modification did not change the spin concentration. The X-band signal has previously been observed to become about 10% narrower in the presence of F^- [11]. NH_3 binding has also been reported to modify the X-band signal by narrowing and shifting its g value to lower field [28], although other researchers have reported that the signal was unchanged by NH_3 [27]; this difference could be due to the presence of different cryoprotectants.

The similar effects of the presence of F^- and NH_3 on the $g = 4$ signal suggests a similar action by these two modifying agents. NH_3, an inhibitor of O_2 evolution, binds to two sites within the OEC [33], one of which is associated with modification of the $g = 4$ signal and the other with modification of the multiline signal [27,28]. Cl^- has been shown to protect one of the NH_3 binding sites [33], that associated with modification of the $g = 4$ signal [28]. F^-, which also inhibits O_2 evolution, competes with amines for the Cl^- binding site [34]. The similarity in the effects of NH_3 and F^- on the signal at $g = 4$ must be related to their occupation of a binding site normally occupied by Cl^-. NH_3 and F^- are both stronger field ligands than Cl^- and would be expected to increase the ZFS of a transition metal ion, which suggests that Cl^-, F^- and NH_3 bind directly to the same position on the Mn center. The effect of such a replacement on the ZFS of an exchange coupled multimer is less clear, however, since only one ion of the cluster may be involved.

The results of this study lead to further speculations on the origins of the S_2-state multiline signal and the signal at $g = 4$. If both signals arise from Mn multimer systems, the relationship between the two signals indicates that they represent two different coupling and/or valence schemes of the same multimer. The observation that the signal at $g = 4$ forms dominantly after illumination at 130–140 K and is partially or completely replaced by the multiline signal upon warming to 200 K [14] strongly suggests that the frozen sample of a dark-adapted OEC is closer to the $g = 4$ signal form than the multiline signal form of the complex. The internal changes in the complex that accompany this EPR change are facilitated (perhaps driven) by additions to the solvent that lower its freezing point (glycerol, ethylene glycol or ethanol). F^- apparently does not allow this conformational change, while sucrose addition gives an intermediate situation. Extrapolating the low-temperature measurements to room temperature, one projects the $g = 4$ signal as characteristic of the S_1-state molecular configuration while the multiline signal is characteristic of the S_2-state molecular configuration. The changes at 200 K are explained as conformational transitions that are allowed by the freedoms associated with the onset of the liquid state. The fact that ammonia binding to the S_1-state has more effect on the $g = 4$ than on the multiline signal is also consistent with this notion.

Acknowledgements

We are indebted to Dr. Tore Vänngård for valuable advice during the preparation of this work. We would like to thank Dr. C.F. Yocum for rewarding discussions and for critically reviewing this work in its final stages, and to him and his co-workers for providing access to O_2 assay equipment. We also thank Ms. W.-W. Zhao for frequent technical assistance. Many thanks to Dr. Ö. Hansson for early help in spectral simulation efforts. We have been grateful for input in the form of discussion from many others during the course of this work. This work was supported by grants from the National Institutes of Health (GM 32785) and the University of Michigan's Office of the Vice President for Research for work performed in the U.S.A., the Swedish Natural Science Research Council and the Axel and Margaret Axson Johnson Foundation for work performed in Sweden, and fellowships to A.H. from the American-Scandinavian Foundation and the University of Michigan's Program in Protein Structure and Design.

References

1 Kok, B., Forbush, B. and McGloin, M. (1970) Photochem. Photobiol. 11, 457–475.
2 Cheniae, G.M. (1980) Methods Enzymol. 69, 349–363.
3 Sauer, K. (1980) Acc. Chem. Res. 13, 249–256.
4 Dismukes, G.C. and Siderer, Y. (1981) Proc. Natl. Acad. Sci. USA 78, 274–278.
5 Zimmermann, J.-L. and Rutherford, A.W. (1986) Biochemistry 25, 4609–4615.
6 Hansson, Ö. and Andréasson, L.-E. (1982) Biochem. Biophys. Acta 679, 261–268.
7 Pecoraro, V.L. (1988) Photochem. Photobiol. 48, 249–264.
8 Dismukes, G.C., Ferris, K. and Watnick, P. (1982) Photobiochem. Photobiophys. 3, 243–256.
9 de Paula, J.C., Beck, W.F. and Brudvig, G.W. (1986) J. Am. Chem. Soc. 108, 4002–4009.
10 Zimmermann, J.L. and Rutherford, A.W. (1984) Biochim. Biophys. Acta 767, 160–167.
11 Casey, J.L. and Sauer, K. (1984) Biochim. Biophys. Acta 767, 21–28.
12 Cole, J., Vittal, K.Y., Gulbes, R.D., McDermott, A.E., Britt, R.D., Dexheimer, S.L., Sauer, K. & Klein, M.P. (1987) Biochim. Biophys. Acta 890, 395–398.
13 Kim, D.H., Britt, R.D., Klein, M.P. and Sauer, K. (1990) J. Am. Chem. Soc. 112, 9389–9391.
14 De Paula, J.C., Beck, W.F., Miller, A.-F., Wilson, R.B. and Brudvig, G.W. (1987) J. Chem. Soc. (Faraday Trans. 1) 83, 3635–3651.
15 Ono, T.-A., Nakayama, H., Gleiter, H., Inoue, Y. and Kawamori, A. (1987) Arch. Biochem. Biophys. 256, 618–624.
16 Hansson, Ö., Aasa, R. and Vänngård, T. (1987) Biophys. J. 51, 825–832.
17 De Paula, J.C., Innes, J.B. and Brudvig, G.W. (1985) Biochemistry 24, 8114–8120.
18 Baumgarten, M., Philo, J.S. and Dismukes, G.C. (1990) Biochemistry 29, 10814–10822.
19 Berthold, D.A., Babcock, G.T. and Yocum, C.F. (1981) FEBS Lett. 134, 231–234.
20 Franzén, L.-G., Hansson, Ö. and Andréasson, L.-E. (1985) Biochim. Biophys. Acta 808, 171–179.
21 Ghanotakis, D.F., Demietriou, D.M. and Yocum, C.F. (1987) Biochim. Biophys. Acta 891, 15–21.
22 Haddy, A., Aasa, R. and Andréasson, L.-E. (1989) Biochemistry 28, 6954–6959.
23 Stevenson, R.C. (1982) Ph.D. thesis, University of Michigan.
24 Aasa, R. and Vänngård, T. (1975) J. Magn. Resonance 19, 308–315.
25 Rutherford, A.W. (1985) Biochim. Biophys. Acta 807, 189–201.
26 Hagen, W.R. (1989) in Advanced EPR (Hoff, A.J., ed.), pp. 785–812, Elsevier, Amsterdam.
27 Beck, W.F. and Brudvig, G.W. (1986) Biochemistry 25, 6479–6486.
28 Andréasson, L.-E., Hansson, Ö. and Von Schenck, K. (1988) Biochim. Biophys. Acta 936, 351–360.
29 Abragam, A. and Bleaney, B. (1970) Electron Paramagnetic Resonance of Transition Ions, pp. 365–471, Dover Publications, New York.
30 Li, Q., Vincent, J.B., Libby, E., Chang, H.-R., Huffman, J.C., Boyd, P.D.W., Christou, G. and Hendrickson, D.N. (1988) Angew. Chem. Int. Ed. Engl. 27, 1731–1733.
31 Nicklin, R.C., Poole, C.P., Jr. and Farach, H.A. (1973) J. Chem. Phys. 58, 2579–2584.
32 Schreurs, J.W.H. (1978) J. Chem. Phys. 69, 2151–2156.
33 Sandusky, P.O. and Yocum, C.F. (1984) Biochim. Biophys. Acta 766, 603–611.
34 Sandusky, P.O. and Yocum, C.F. (1986) Biochim. Biophys. Acta 849, 85–93.
35 Aasa, R. (1970) J. Chem. Phys. 52, 3919–3930.